Food & Function

PAPER

View Article Online
View Journal | View Issue

Cite this: *Food Funct.*, 2015, **6**, 1796

Calcium bioaccessibility and uptake by human intestinal like cells following *in vitro* digestion of casein phosphopeptide–calcium aggregates

Silvia Perego,†[a] Elena Del Favero,[b] Paola De Luca,[a] Fabrizio Dal Piaz,[c] Amelia Fiorilli,[a] Laura Cantu'[b] and Anita Ferraretto*[a]

Received 28th July 2014,
Accepted 18th April 2015

DOI: 10.1039/c4fo00672k

www.rsc.org/foodfunction

Casein phosphopeptides (CPPs), derived by casein proteolysis, can bind calcium ions and keep them in solution. *In vitro* studies have demonstrated CPP-induced cell calcium uptake, depending on the formation of (CPP + calcium) complexes and on the degree of differentiation of the intestinal cells. With the present study, we address the persistence of the complexes and of the CPP-induced calcium uptake in intestinal like cells after the digestion process, thus examining their eligibility to serve as nutraceuticals. A calcium-preloaded CPP preparation of commercial origin (Ca–CPPs) was subjected to *in vitro* digestion. The evolution of the supramolecular structure of the Ca–CPP complexes was studied using laser-light and X-ray scattering. The bioactivity of the pre- and post-digestion Ca–CPPs was determined in differentiated Caco2 and HT-29 cells by video imaging experiments using Fura-2. We found that Ca–CPP aggregates keep a complex supramolecular organization upon digestion, despite getting smaller in size and increasing internal calcium dispersion. Concomitantly and most interestingly, digested Ca–CPPs clearly enhance the uptake of calcium ions, especially in Caco2 cells. In contrast, digestion depletes the ability of post-loaded decalcified-CPPs (Ca–dekCPPs), with a weaker internal structure, to induce calcium uptake. The enhanced bioactivity reached upon digestion strongly suggests a recognized role of Ca–CPPs, in the form used here, as nutraceuticals.

1. Introduction

The retention or acquisition of a specific biological activity after the digestion process is a prerequisite to define a "functional food". This essential property is mostly due to the presence of specific molecules, identified or not, contained in the food and released mainly by the digestion process. Milk proteins represent a good example of this possibility, since they constitute a source of many biologically active peptides exerting their bioactivity at different physiological levels.[1,2] Therefore, dairy products can be fully considered as functional foods and the bioactive molecules present inside as nutraceuticals.

Numerous studies have investigated the persistence of milk-derived peptides both after the *in vitro* digestion[3–5] and *in vivo* in the intestine of humans.[6,7] The next step, therefore, is to demonstrate that, although eventually modified by digestion, these peptides and especially their bioactive aggregated complexes can retain or even acquire their biological capacity. Due to the diverse chemico-physical structure and function displayed by the different milk-derived peptides, it is likely that both their resistance to proteolysis and their bioactivity could be non-uniform, according to the experimental and/or physiological conditions.[5]

In the present paper we deal with the casein phosphopeptides (CPPs), derived by casein proteolysis, which have the ability to bind calcium ions, include them in complexes and keep them in solution.[8]

In vitro studies, using human intestinal cell models, have demonstrated the involvement of CPPs in cell calcium uptake, depending on the formation of (CPP + calcium) aggregates[9] and on the degree of differentiation of the intestinal cells.[10] It is noteworthy that the calcium uptake triggered by CPPs in the two intestinal human *in vitro* cell models used, namely, differentiated Caco2 and HT-29 cells, involves two different mechanisms at the membrane level. In HT-29 cells, calcium uptake occurs *via* the depolarizing L-type calcium channels. Instead, in Caco2 cells, it involves the transient receptor potential cation of the vanilloid subfamily V member 6, TRPV6 channel,

[a]*Dipartimento di Scienze Biomediche per la salute, Università degli Studi di Milano, LITA, via Fratelli Cervi 93, Milano, Italy. E-mail: anita.ferraretto@unimi.it; Fax: +39 0250230452; Tel: +39 0250330341*
[b]*Dipartimento di Biotecnologie Mediche e Medicina Traslazionale, Università degli Studi di Milano, LITA, via Fratelli Cervi 93, Milano, Italy*
[c]*Dipartimento di Farmacia, Università degli Studi di Salerno, Italy*
† Present address: IRCCS Istituto Ortopedico Galeazzi, via R. Galeazzi 4, 20161, Milano, Italy.

also designated as calcium transporter-1 or CaT1.[11,12] Both channels are recognized to exert an active role in intestinal calcium absorption, although with important differences regarding vitamin D regulation, the intestinal tract of interest, and the condition of activation/inactivation (by depolarization or hyperpolarization).[11]

The interaction of CPPs with these channels, promoting calcium uptake, also affects cell proliferation and apoptosis, through the role exerted by calcium ions themselves in these processes, a property which could have potential implications to the tumour/normal cell phenotype.[13–15] Also on this basis, it is of paramount interest to prove that CPPs can behave as nutraceuticals, keeping their features and bioactivity after their localization in the intestine.

It is known that the digestion of casein micelles, the form with which casein is bound to calcium ions in milk, gives rise to complexes containing calcium phosphate and CPPs, namely α_{s1}-CPP and β-CPP, displaying different binding properties for calcium and phosphate, as compared to casein.[16]

The present study is devoted to assessing the eligibility of CPPs to serve as nutraceuticals. To address this issue, the bioaccessibility of the (CPP + calcium) complexes was analysed in cultures of intestinal human cells. The bioavailability of the same calcium–CPP complexes has been studied in the past and positively established by means of experiments in humans[17,18] identifying a positive effect on calcium and zinc absorption, together with a recognized mineral bioavailability in rat pups.[19] Calcium–CPP complexes have shown up to be bioactive also at the bone level. In fact, the ingestion of calcium–CPP complexes inhibited the bone loss in aged ovariectomized rats[20] and supplementation with CPPs of different origins increased calcification of the diaphyseal area of explanted rat bone rudiments *in vitro*.[21] Another recognized positive effect of CPPs is at the dental level, with an anticariogenic role due to the increase of the plaque level of calcium phosphate.[22,23]

The present study is therefore conceived to verify the persistence, along and after a simulated digestion, (i) of the CPP-calcium aggregates (the bioactive form) and (ii) of their ability to induce the calcium uptake by the cells, a feature that was demonstrated in a previous study.[24] We underline that we focus on calcium uptake connected to ion transport, by selecting suitable, short, observation times. Any concern to the peptide transport is outside the scope of our study. Great care was taken to ensure that all the measurements, both structural (i) and biological (ii), were performed under the same experimental conditions (the peptide/calcium molar ratio and the absence of inorganic phosphate in the solution) for punctual comparison. All the experiments were performed on a CPP preparation, characterized in a previous study, consisting of a mixture of peptides (mainly from the N-terminus of beta casein, but also from alpha s1 casein) already calcium-containing (6.6% w/w), roughly corresponding to 1.5 calcium ions per organic phosphate (3.2% w/w) and particularly resistant to variations in the (possibly random) environmental calcium ion concentration,[24] hereafter Ca–CPPs. The same experiments were also carried out using complexes obtained by post-loading calcium to the decalcified form of the same CPPs (hereafter Ca–dekCPPs). In fact, dekCPP has been proved to be very efficient in complexing all of the available calcium ions,[24] thus it may be suitable as a high-performing nutraceutical, considering that after a meal CPPs come in contact with a huge amount of calcium.[25]

2. Materials and methods

2.1. Materials and reagents

Cell culture media, L-glutamine, antibiotic–antimycotic solution, sodium pyruvate, trypsin-EDTA solution, EGTA and all other reagents, unless otherwise specified, were purchased from Sigma-Aldrich (St. Louis, MO, USA). Foetal bovine serum (FBS) was from EuroClone Ltd (West Yorkshire, UK). Fura-2 acetoxymethyl ester (Fura-2/AM) was from Calbiochem (La Jolla, CA, USA).

2.2. Casein phosphopeptides (CPPs)

The CPP preparation (Peptigen®110) used here was kindly provided by MD Foods Ingredients Amba (Videbaek, Denmark) and represents a purified tryptic casein hydrolysate containing a very high level of CPPs. This preparation was previously studied for it concerns product quality parameters such as calcium content, CPP and protein content, Ser/P ratio[26] and the ability to induce calcium uptake in intestinal cells.[24] The MALDI-TOF/MS analysis[24] identified two main components, an N-terminal tryptic peptide 1–25, obtained from beta casein, bearing four phosphate groups, and a 62–79 peptide obtained from alpha s1 casein, with three phosphate groups. Based on the size distribution given by the MS spectra, the average molecular weight was assumed to be 2500.[24] Its composition from the manufacturing data sheet, which is in accordance with data published,[26] is the following: 95% CPP content; 6.6% calcium content; 3.2% phosphorus content; N/P ratio: 7.8 mol mol^{-1}; Ser/P ratio: 0.97 mol mol^{-1}. CPP solutions used in all the experiments were prepared at 1280 μM peptide concentration, corresponding to the maximum activity in inducing the intracellular calcium rise.[9,10,24] As a main feature, these CPPs, hereafter Ca–CPPs, contain calcium at the origin, in the stock powder preparation. As determined previously,[24] a fraction of the pre-loaded calcium is stably associated with Ca–CPP complexes, an amount nicely independent of the extra calcium present in the solution.

An aliquot of Ca–CPPs was decalcified, by the chelating ion exchange resin Chelex100 (Bio-Rad Laboratories, Hercules, CA, USA), according to the procedure already described.[24] This second CPP preparation was named dekCPP, in opposition to its parent Ca–CPP, and Ca–dekCPP after dissolution in a calcium-containing solvent. In order to prepare the Ca–dekCPP complexes, calcium was added with the solvent used to solubilize the dekCPP powder.

2.3. *In vitro* digestion of Ca–CPPs and Ca–dekCPP

Enzymes and bile salts were purchased from Sigma-Aldrich (St. Louis, MO, USA). 40 mg of porcine pepsin (EC 3.4.23.1, catalog no. P-7000) was suspended in 1 mL of 0.1 N HCl; 20 mg of pancreatin (catalog no. P-1750) and 120 mg bile extract (catalog no. B-8631) were dissolved in 10 mL of 0.1 M $NaHCO_3$.

3 mL of double distilled water were added to 500 mg of Ca–CPPs (50× concentrated, with respect to the final concentration) and the pH was adjusted to 2 with 5 M HCl. The same procedure was applied to dekCPPs, but calcium was also added, as $CaCl_2$, in order to reproduce the amount embedded in Ca–CPP complexes (two calcium ions per peptide chain). The two samples were then subjected in parallel to simulated digestion, as follows. 5 mg of freshly prepared pepsin solution were added, and the samples were incubated in a shaking water bath at 37 °C for 90 min. The gastric digests were then kept in ice for 10 minutes to stop the pepsin digestion. Prior to the intestinal digestion step, the pH of the gastric digests was raised to 6 by dropwise addition of 1 M $NaHCO_3$. Successively, 8.75 mg of the pancreatin–bile extract mixture were added and the incubation was continued for an additional 2 h. After that, the samples were put in an ice bath for 10 min to stop the intestinal digestion. The pH was adjusted to 7.2 by dropwise addition of 0.5 M NaOH. The intestinal digests were heated for 4 min at 100 °C to inhibit proteases and then immersed in an ice bath to cool. Then, aliquots of 1 mL of the samples were transferred to centrifuge tubes polyallomer® (Beckman Coulter, Brea, CA, USA) and centrifuged at 12 000*g* for 30 min at 4 °C (TL-100 Ultracentrifuge, Beckman Coulter). The supernatants were transferred and pooled at −20 °C. Finally, water was added to adjust the osmolarity to 300 ± 20 mOsm kg^{-1} (cryoscopic osmometer Osmomat 030, Gonotec GmbH, Berlin, Germany).[27,28]

Both the initial and the digested final samples of both CPPs were subjected to the Lowry protein assay,[29] showing a protein recovery of 82%.

2.4. LC/MS/MS analysis

Peptides were analyzed by LC/MS/MS using an Orbitrap XL instrument (Thermo Fisher, Waltham, MA, USA) equipped with a nano-ESI source coupled with a nano-ACQUITY capillary UPLC (Waters, Milano, Italy): peptide separation was performed on a capillary BEH C18 column (0.075 mm × 100 mm, 1.7 μm, Waters) using aqueous 0.1% formic acid (A) and CH_3CN containing 0.1% formic acid (B) as mobile phases. Peptides were eluted by means of a linear gradient from 5% to 50% of B in 45 min and a 300 nL min^{-1} flow rate. Mass spectra were acquired over an m/z range of 400–1800; the ten most intense doubly-, triply- or quadruply-charged ions detected in each spectrum underwent CID fragmentation (dependent scan acquisition mode) and MS/MS spectra were acquired over an m/z range of 50–2000. MS and MS/MS data were used by Mascot (Matrix Science, London, UK) to interrogate the Swiss-Prot protein database. Settings were as follows: taxonomy, other mammalia; enzyme, no cleave; mass accuracy window for parent ions, 10 ppm; mass accuracy window for fragment ions, 50 millimass units; no fixed modification; variable modifications, phosphorylation of serine, threonine and tyrosine, oxidation of methionine.

2.5. Laser light scattering

Aliquots of CPPs, dissolved in pure water as concentrated stocks, were diluted in phosphate-free KRH with calcium at concentrations matching those used to monitor the CPP biological effect. The laser light scattering apparatus has been designed in our laboratories (Department of Medical Biotechnology and Translational Medicine, University of Milan) to be quite sensitive, thanks to four optical channels. It includes a diode laser (λ = 532 nm) and a temperature controlled cell. Both independent static (SLS) and dynamic (QELS) laser light scattering measurements were performed on each sample at room temperature. Dynamic measurements, through the correlation function of the scattered intensity, yield the translational diffusion coefficients of particles in solution and then, *via* the Stokes–Einstein relation, their average hydrodynamic diameter. By parallel static measurements of the average scattered intensity, information on the mass of particles in solution were obtained.

2.6. Small angle X-ray scattering (SAXS)

SAXS measurements were performed at the ID02 high-brilliance beamline at the ESRF (Grenoble, France), with a beam cross section of 0.3 mm × 0.8 mm and a wavelength of 0.1 nm, in the region of momentum transfer, $q = (\pi/\lambda)\sin(\theta/2)$, 0.017 $nm^{-1} \leq q \leq 4.65$ nm^{-1}, where θ is the scattering angle. All measurements were performed at room temperature with a very short exposure time, 0.1 s, in order to avoid any radiation damage. Samples were put in plastic capillaries (KI-beam, ENKI, Concesio, Italy) mounted horizontally onto a six-places sample holder, allowing for nearly contemporary measurements on sample and reference cells. The measured SAXS profiles report the scattered radiation intensity $I(q)$ as a function of the momentum transfer, q. Several spectra relative to the empty cells and the solvent were taken, carefully compared and subtracted to each sample spectrum. A SAXS analysis was carried out to assess the structure of the particles in solution on a more local, internal, scale with respect to laser light scattering analysis. The experimental $I(q)$ profile was then fitted with the internal form factor (P_{Int}) characteristic of structures obtained by random condensation of functional monomers, in which the resulting statistic of the subchains is Gaussian. For equal reaction probability of the functional groups: $P_{Int} = 1/(1 + \langle R_g^2\rangle q^2/3)$,[30] where $\langle R_g^2\rangle$ is the average radius of gyration squared of the subchain, proportional to the correlation length within the entanglement network. We also tested the model developed for the internal structure of casein micelles, which consists of calcium phosphate nanoparticles reticulated in the peptide matrix.[31] This model is not suitable for the internal structure of CPP aggregates and has been discarded.

2.7. Cell culture

The human colon adenocarcinoma cell lines Caco2 (BS TCL 87) and HT-29 (BS TCL 132) were supplied by Istituto Zooprofilattico Sperimentale di Brescia (Brescia, Italy).

Caco2 cells were cultured in 75 cm^2 plastic flasks (VWR International PBI, Milan, Italy) in EMEM (Minimum Essential Medium Eagle's) growth medium supplemented with 15% heat-inactivated foetal bovine serum (FBS), 1 mM sodium pyruvate, 2 mM L-glutamine, 0.1 mg L^{-1} streptomycin, 1×10^5 U L^{-1} penicillin, and 0.25 mg L^{-1} amphotericin-B. The differentiation of Caco2 cells was achieved according to the well-established procedure[32] consisting of successive sub-cultivations without reaching the post-confluent stage.

HT-29 cells were grown (75 cm^2 plastic flasks, VWR International PBI) in RPMI 1640 medium (Roswell Park Memorial Institute), supplemented with 10% heat-inactivated foetal bovine serum, 2 mM L-glutamine, 0.1 mg L^{-1} streptomycin, 1×10^5 U L^{-1} penicillin, and 0.25 mg L^{-1} amphotericin-B, obtaining a population of differentiated and polarized cells, although with a high degree of heterogeneity.[33]

All cell cultures, kept at 37 °C under a 5% CO_2–95% air atmosphere, were periodically checked for the presence of mycoplasma and were found to be free of contamination.

2.8. Measurement of cytoplasmic calcium content, $[Ca^{2+}]_i$, at the single-cell level

Cytoplasmic calcium, $[Ca^{2+}]_i$, was measured in cells seeded on glass coverslips (∅ = 24 mm) and loaded with 2.5 μM Fura-2/AM and 2.5 μM Pluronic F-127, in phosphate-free Krebs Ringer HEPES solution (KRH, 140.0 mM NaCl, 5.0 mM KCl, 2 mM $CaCl_2$, 0.55 mM $MgCl_2$, 6.0 mM glucose and 10.0 mM HEPES, pH 7.4) as previously described.[9–11,34] Fluorescence determination was performed with a microscope (TE 200, Nikon, Tokyo, Japan) connected to a CCD intensified camera (Extended Isis, Photonic Science, Millham, UK) and to a thermostatted (TC-202 A, Medical System Corporation, Harvard Apparatus, Holliston, MA, USA) perfusion chamber (PDMI-2, the same commercial source). The amount of intracellular free calcium, $[Ca^{2+}]_i$, within every single cell, was calculated using a fluorescence image acquisition and data analysis system (Applied Imaging, High Speed Dynamic Video Imaging Systems, Quanticell 700, Sunderland, UK) from the 340/380 nm images, using a calibration performed with external standards of calcium and Fura-2, according to the equation reported in ref. 35. Fig. 5 and 6 show one representative experiment from 6–8 replicates (the number of technical replicates) for each of the following samples: Ca–CPPs, digested Ca–CPPs, Ca–dekCPPs and digested Ca–dekCPPs. In each experiment, 70–90 cells were analysed (biological replicates). Fig. S1 and S2 in the ESI† show the average behaviour plus the standard deviation from all the replicates. The average values for all the technical replicates for each sample were reported as: (i) percent of cells responding to CPP administration with an increment in the intracellular calcium concentration; (ii) the mean single-cell $[Ca^{2+}]_i$ rise, namely, the difference between the maximum and the basal values of $[Ca^{2+}]_i$ for each cell, averaged over the analysed cell population ($\Delta[Ca^{2+}]_i$), composed of 400 Caco2 cells and 500 HT-29 cells; (iii) the total $[Ca^{2+}]_i$ rise ($tot[Ca^{2+}]_i$), obtained by multiplying the percent of responsive cells by the mean single $[Ca^{2+}]_i$ rise ($\Delta[Ca^{2+}]_i$).

2.9. Statistical analysis of cell population

To determine statistically significant differences ($p < 0.005$ or $p < 0.01$), the results obtained were analyzed by Student's *t*-test, independent two population test and χ^2 test.

3. Results

The results obtained by the two parallel sets of experiments, structural and biological, are reported separately in the following, for clearer description, and then merged in the discussion.

3.1. Structural results

3.1.1. LC-ESI-MS/MS results. In Table 1 the main molecular mass peptides derived from the *in vitro* digestion of CPPs are listed, as identified by their molecular mass. A number of short peptides from beta and alpha s1 casein were detected, most of which comprise one or more phosphorylated serines. In particular, the peptides from beta casein are more abundant than those of alpha s1 casein and they are constituted by a smaller number of amino acids. Peptides from beta casein derived mainly from the N-terminus portion as 1–25 or 33–55 polypeptide chain, while those from alpha casein derived from the alpha 110–119 portion.

3.1.2. Laser light scattering results. Laser light scattering measurements were performed to characterize the Ca–CPP and Ca–dekCPP supramolecular complexes on the colloidal length-scale and to follow their possible disaggregation upon digestion. These aggregated structures are formed due to the interaction between negatively charged phosphorylated serines and positive divalent calcium ions. In the present work, before digestion (pH 7.4), the fraction of calcium embedded within the aggregates is the same for both Ca–CPPs and Ca–dekCPPs, namely ~2 Ca/CPPs mole/mole, as recalled before. The presence of aggregated structures is essential for the bioactivity of CPPs, as the fraction of calcium internalized by cells is actually the CPP-complexed calcium.[9,24] Before digestion, both CPPs form aggregates with a similar average hydrodynamic radius and quite a high polydispersity (140 ± 25 nm).

In order to follow the evolution of the supramolecular complexes during the digestion process, we designed two experiments. In the first experiment, we simply changed the pH of the solution, from pH 7.4 down to pH 2 and back to neutral pH. The average overall size of the complexes was determined at the different stages of the experiment. Although obtained in the absence of digestive enzymes, these results may be fundamental to understand the behaviour of the supramolecular complexes. In fact, CPPs, produced by tryptic hydrolysis of sodium caseinate[24] in the commercial product used here, are

Table 1 LC-ESI-MS/MS based identification of the main molecular mass peptides from the enzymatically digested CPP sample

Parent protein	Position	Observed	M_r (expt)	M_r (calc.)	ppm	Peptide
Beta casein	1–6	394.7117	787.4078	787.4075	0.65	A.RELEEL.N
Beta casein	1–11	642.8264	1283.6362	1283.6357	0.98	A.RELEELNVPGE.I
Beta casein	1–16	953.4642	1904.9138	1904.9132	0.34	A.RELEELNVPGEIVESL.S + Phospho (S)
Beta casein	4–11	443.7116	885.4086	885.408	0.78	L.EELNVPGE.I
Beta casein	6–14	485.2662	968.5178	968.5179	−0.0052	E.LNVPGEIVE.S
Beta casein	6–16	625.3076	1248.6006	1248.6003	0.31	E.LNVPGEIVESL.S + Phospho (S)
Beta casein	7–16	568.7657	1135.5168	1135.5162	0.57	L.NVPGEIVESL.S + Phospho (S)
Beta casein	30–44	974.3999	1946.7792	1946.7782	1.61	K.IEKFQSEEQQQTEDE.L + Phospho (S)
Beta casein	33–45	845.8281	1689.6416	1689.6407	0.57	K.FQSEEQQQTEDEL.Q + Phospho (S)
Beta casein	33–48	1031.4194	2060.8242	2060.8212	1.5	K.FQSEEQQQTEDELQDK.I + Phospho (S)
Alpha s1 casein	41–70	971.2587	3881.0457	3881.0514	−0.5	L.SKDIGSESTEDQAMEDIKQMEAESISSSEE.I + 2 Oxidation (M); 7 Phospho (S)
Alpha s1 casein	43–58	972.3469	1942.6792	1942.6792	0.033	K.DIGSESTEDQAMEDIK.Q + oxidation (M); 2 Phospho (S)
Alpha s1 casein	109–118	590.7621	1179.5066	1179.506	1.08	Q.LEIVPNSAEE.R + Phospho (S)
Alpha s1 casein	110–118	534.2196	1066.4226	1066.422	0.53	L.EIVPNSAEE.R + Phospho (S)

similar to those produced by the enzymes operating along the physiological digestive process. In the second experiment, we followed the *in vitro* digestion protocol described in the Materials and methods section, adding enzymes to the CPPs at the appropriate pH values. Laser light scattering experiments were performed on CPP solutions at the beginning, after acidification and/or pepsin addition, and at the end of the process.

The measured size distribution of the CPP complexes at different pH values, characteristic of each digestion step, for both Ca–CPP (left side) and Ca–dekCPP (right side), is reported in Fig. 1. The complexes are classified into three size ranges (tens, hundreds and thousands of nm) and their relative importance is reported as relative scattered intensity. Results in Fig. 1 clearly show that, as compared to the initial stage (left bar in both groups), upon acidification the distribution shifts to smaller size (tens of nm) for both systems (central bar). As the pH is raised again, large aggregates quickly reform (right bar). This general behaviour is displayed by both systems.

Results relative to the experiment performed on CPP solutions in the presence of different enzymes, pepsin and pancreatin at different pH, showed that the evolution of the overall size of the complexes is qualitatively similar. A detailed assessment of the size distribution of the CPP complexes, in this case, is prevented by the interference of the scattered intensity coming from the enzyme preparations themselves.

3.1.2. SAXS results. The internal structure of CPP complexes and its evolution during the digestion process were assessed by SAXS measurements. Spectra are reported in Fig. 2, for both Ca–CPPs and Ca–dekCPPs, at the three stages of simulated digestion, as before. The X-ray scattered-intensity profile, in the high-q region, corresponding to short distances within the aggregate (local structure), is similar for all spectra, showing a q^{-2} decay of $I(q)$. This behaviour is characteristic of non-globular objects with fractal or entangled chain-like conformation. In the low-q region, corresponding to longer distances, the intensity profiles display a slight increase, relative to the overall structure of the aggregates, typically assessed by light scattering, as above. Those results on the structure of CPP complexes, although apparently not so far from the ones obtained on casein micelles,[31,36–40] nonetheless unravel interesting differences regarding the sites of calcium inclusion, connected to the absence, in Ca–CPPs, of excess phosphate, as we will point out in the Discussion section.

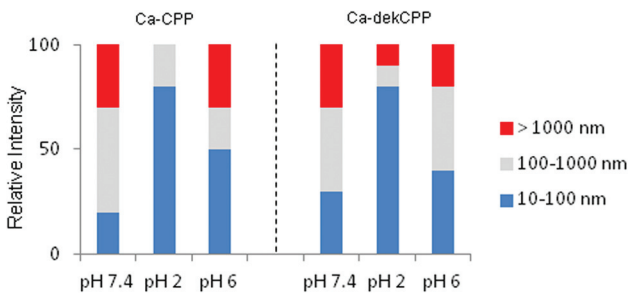

Fig. 1 Size distribution of Ca–CPP (left side) and Ca–dekCPP (right side) complexes at different pH values, characteristic of each digestion step: initial, pH 2, pH 6. The complexes are classified as belonging to three size-ranges (tens, hundreds and thousands of nm) and their relative importance is expressed as relative scattered intensity (%).

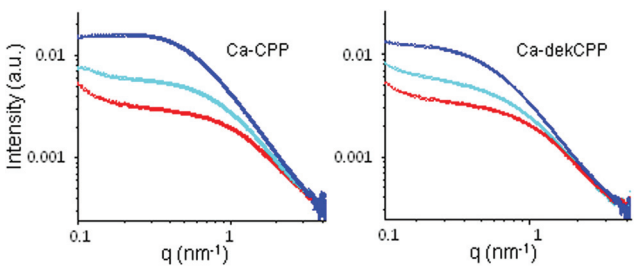

Fig. 2 Ca–CPP (left) and Ca–dekCPP (right) SAXS spectra at different digestion steps: the initial state (blue), after gastric phase (cyan), and after intestinal phase (red). A shoulder is visible in the intensity profile corresponding to the initial state of Ca–CPPs. In the other spectra, the intensity profiles at low q display a slight increase, a sign of the aggregates' overall structure.

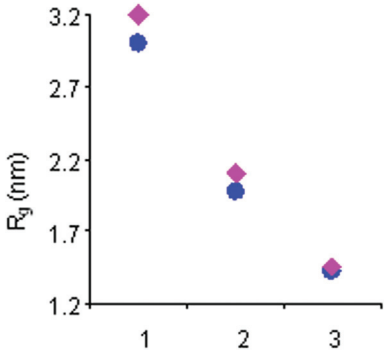

Fig. 3 Ca–CPP (blue) and Ca–dekCPP (magenta) local structures. Radius of gyration of the subchains within the entanglement network at different digestion steps: (1) initial, (2) after acidification and pepsin action, and (3) after pancreatin action at pH 6.

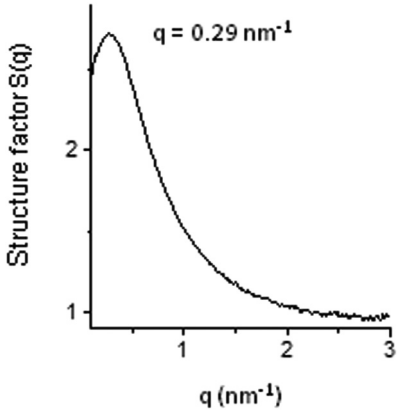

Fig. 4 Experimental structure factor $S(q)$ for Ca–CPPs under the initial conditions. The peak at q = 0.29 nm^{-1} indicates the presence of inter-chain interactions that assume a preferential distance in the entangled phase. The characteristic length is d = 22 nm.

Analysis of the scattered intensity has been performed following the model described in the Materials and methods section. We also tested and rejected the model developed for the internal structure of casein micelles, characterized by calcium phosphate nanoparticles reticulated in the peptide matrix.[31] The internal structure of the (CPP + calcium) complex was modelled as a collection of randomly condensing monomers. These monomers, the peptide chains, entangle thanks to the interaction of negatively-charged phosphorylated-serine residues and divalent positive calcium ions. On a local length scale, small compared to the mesh size of the entangled network, we could observe the structure of the individual flexible subchains. Results on the average radius of gyration of the subchains for the Ca–CPPs and Ca–dekCPPs are reported in Fig. 3 at different digestion steps: the initial condition (1), after acidification and pepsin action (2), and after pancreatin action (3).

In addition, in the SAXS intensity profile relative to the Ca–CPP sample in its initial state, a shoulder is clearly visible, a signature of a structure factor. The experimental structure factor, reported in Fig. 4, shows a peak (q_{peak} = 0.29 nm^{-1}) confirming the presence of inter-chain interactions between peptides that, in the entangled phase, assume a preferential distance (d = 22 nm). Interestingly, after acidification and pepsin addition, this structure peak disappears, indicating that the internal structure of the Ca–CPP complexes becomes more flexible and irregular.

3.2. Biological results

The changes in the intracellular calcium concentration, $[Ca^{2+}]_i$, induced by both Ca–CPPs and Ca–dekCPPs and their digested counterparts, all containing the same amount of calcium, were evaluated and analysed in differentiated Caco2 and HT-29 cells. An example of the profiles of the single cell responsiveness to CPPs is reported in Fig. 5 and 6, while the average cell response plus the standard deviation is reported in Fig. S7 and S8 in the ESI.† The effects of the different administrations, expressed as percent of the responsive cells, together with the increment in the cytoplasmic calcium concentration ($\Delta[Ca^{2+}]_i$), for any single cell and for the whole cell population (tot $[Ca^{2+}]_i$), are reported in Tables 2 and 3.

In Caco2 cells (see Fig. 5 and Table 2) the administration of the digested Ca–CPP instead of its undigested counterpart produces calcium uptake in a higher fraction of cells (70% *vs.* 15%), as well as a higher increase in the intracellular calcium concentration ($\Delta[Ca^{2+}]_i$, 45 ± 10 nM *vs.* 27 ± 9 nM). Between the undigested forms, Ca–dekCPP is more effective than Ca–CPP, both as a fraction of responding cells (26% *vs.* 15%) and as a $[Ca^{2+}]_i$ increase (40 ± 20 nM *vs.* 27 ± 9 nM). Digestion of Ca–dekCPP does not significantly alter the single-cell increment in calcium uptake ($\Delta[Ca^{2+}]_i$), despite occurring in a smaller population of cells (18% *vs.* 26%). Interestingly, when digested complexes are supplied, the recovery of the intracellular calcium basal level occurs on much longer time scales, roughly fourfold. This feature is common to both Ca–CPPs and Ca–dekCPPs.

In HT-29 cells (see Fig. 6 and Table 3), again, the administration of the digested Ca–CPP produces a cellular response significantly higher than that produced by its undigested counterpart, both as a fraction of responsive cells (89% *vs.* 70%) and in the intracellular calcium increase (115 ± 19 nM *vs.* 76 ± 28 nM). Administering the undigested Ca–dekCPP, as reported previously,[24] induced calcium uptake in a higher number of cells with respect to Ca–CPP (93% *vs.* 70%), with an overall extent reached by Ca–CPPs only after digestion. Reversely, digestion reduces the effectiveness of Ca–dekCPPs to promote single-cell calcium uptake (from 113 ± 59 to 79 ± 14 nM), although acting on the same fraction of cells (96% *vs.* 93%). The kinetic profiles of the intracellular calcium concentration show the same features observed in Caco2 cells, *i.e.*, a slower recovery of the basal level and a higher heterogeneity in the cell behaviour in the case of digested CPPs.

As a whole, these data indicate that digestion of Ca–CPPs results in an increment both in the number of cells respond-

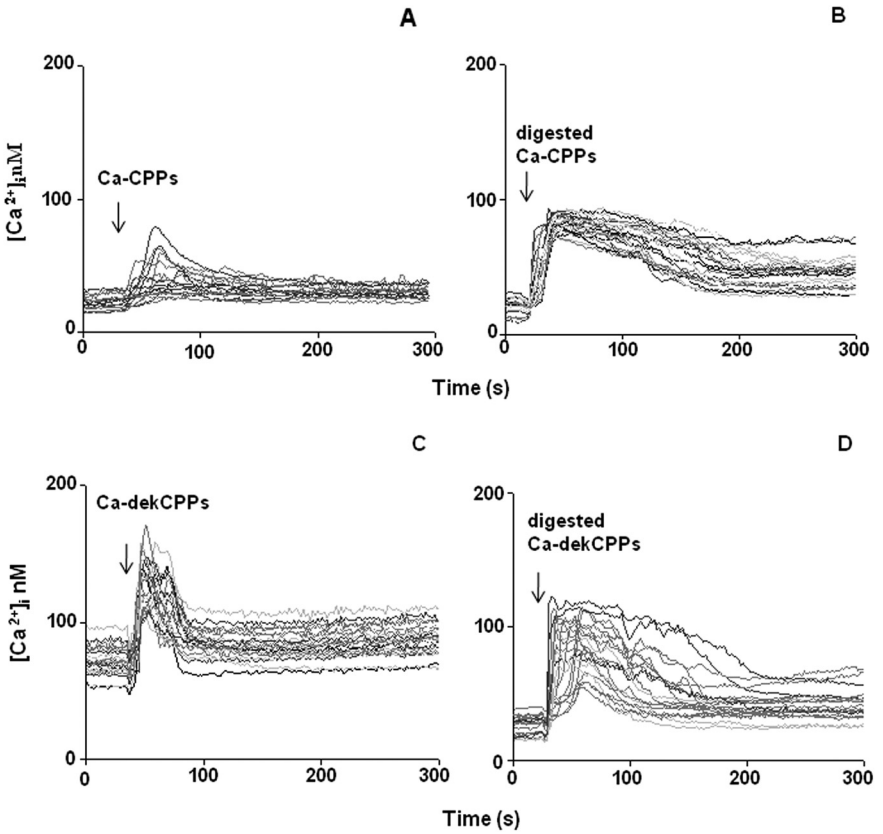

Fig. 5 Effect of CPPs in Caco2 cells. The average change in cytosolic calcium, $[Ca^{2+}]_i$, after administration (1280 μM) of Ca–CPPs (A), digested Ca–CPPs (B), Ca–dekCPPs (C) and digested Ca–dekCPPs (D) together with relative SD is shown. Each graph represents the average behaviour of 10–12 independent experiments, each of them consisting of a minimum of 40–60 analysed cells.

ing with a calcium rise and in the amount of calcium taken up by each cell, ($\Delta[Ca^{2+}]_i$). The increase of the total intracellular calcium concentration reached after the administration of digested Ca–CPPs (tot $[Ca^{2+}]_i$) as compared to its undigested counterpart is notably higher in Caco2 cells (778%) as compared to HT-29 cells (192%), beyond the absolute values of the single measures in the two cell lines. Reversely, in the case of Ca–dekCPP, the digestion procedure depletes the overall increase in calcium uptake (tot $[Ca^{2+}]_i$), through a reduction either in the number of responsive cells or in the single-cell calcium increase, depending on the cell type. In both cases, a reduction to less than 80% in effectiveness is observed (78% in Caco2 cells and 72% in HT-29 cells) (Table 2 and 3).

4. Discussion

Bioactive peptides released by the gastrointestinal digestion of food proteins can exert biological properties in addition to the well-known nutritional ones, both soon after digestion, mainly toward intestinal cells, and after their absorption by the intestine, when they have reached their specific targets in the body. Digestion and absorption are limiting steps for the bioavailability of peptides; thus the *in vitro* digestion procedures combined with the use of intestinal cell models allowed to mimic the physiological milieu, where digestion occurs, and the interactions between peptides and intestine, the latter representing the first contact between food and our body.[41]

The potentiality of the casein phosphopeptides has been evidenced in recent publications.[10,11] In this context, the present paper addresses the modifications occurring in the structure of (CPP + calcium) aggregates at the various digestion steps (*in vitro* procedure), concerning their complexation with calcium ions, in relation to the effect on their ability to induce calcium uptake by intestinal cells, without any concern about the peptide transport, which is outside the scope of the present study.

The *in vitro* digestion of CPPs gives rise to a mixture of peptides from beta and alpha s1 casein, mostly composed of 5–15 amino acids, with one or more phosphoserines. Moreover, the fragment 41–70 from alpha s1 casein contains the phosphorylated acidic motif SSSEE. Although showing increased fragmentation with respect to the undigested CCPs, this peptide pattern is consistent with the ability to bind calcium ions, the property specifically addressed here. In this sense, the first aspect to be evaluated was the persistence of the CPP aggregates with calcium ions even after digestion, since this is fundamental to promote any calcium uptake by the cells.[24]

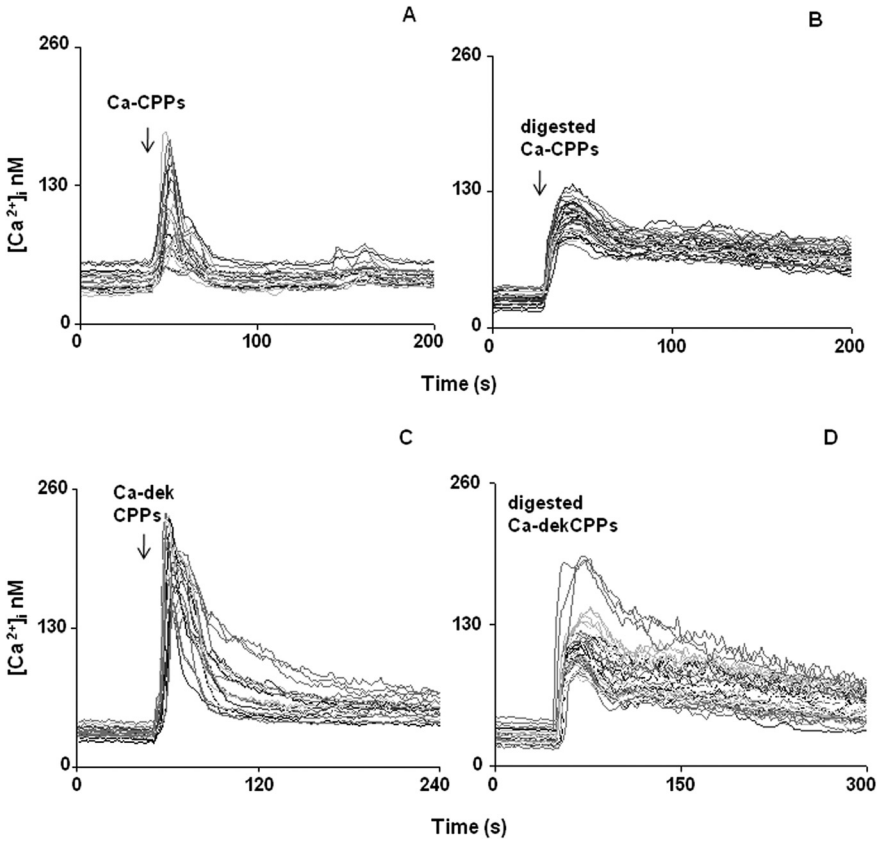

Fig. 6 Effect of CPPs in HT-29 cells. The average change in cytosolic calcium, $[Ca^{2+}]_i$, after administration (1280 μM) of Ca–CPPs (A), digested Ca–CPPs (B), Ca–dekCPP CPPs (C) and digested Ca–dekCPPs (D) together with relative SD is shown. Each graph represents the average behaviour of 10–12 independent experiments, each of them consisting of a minimum of 70–90 analysed cells.

Table 2 Statistical analysis of Ca–CPP and Ca–dekCPP effects on calcium uptake in Caco2 cells before and after the simulated digestion process[a]

Treatments	% Responsive cells	$\Delta[Ca^{2+}]_i$ (nM)	tot $[Ca^{2+}]_i$ (nM)
Ca–CPPs	15	27 ± 9	405
Digested Ca–CPPs	70°	45 ± 10*	3150
Ca–dekCPPs	26°	40 ± 20*	1040
Digested Ca–dekCPPs	18^$	45 ± 13*	810

[a] The statistical significance for cell responsiveness (% responsive cells) was assessed using the χ^2 test: significantly different from Ca–CPP (°, $p < 0.005$); from digested Ca–CPP (^, $p < 0.005$); from Ca–dekCPPs ($, $p < 0.005$). The variations in the average single-cell intracellular calcium concentration ($\Delta[Ca^{2+}]_i$) were analyzed by Student's *t*-test (*significantly different from Ca–CPPs, $p < 0.01$). Each value represents the mean ± SD of 10–12 analogous experiments for at least 400 analyzed cells. Details of the calculations are reported in the Materials and methods section.

Table 3 Statistical analysis of Ca–CPP and Ca–dekCPP effects on calcium uptake in HT-29 cells before and after the simulated digestion process[a]

Treatments	% Responsive cells	$\Delta[Ca^{2+}]_i$ (nM)	tot $[Ca^{2+}]_i$ (nM)
Ca–CPPs	70	76 ± 28	5320
Digested Ca–CPPs	89°	115 ± 19*	10 235
Ca–dekCPPs	93°	113 ± 59	10 509
Digested Ca–dekCPPs	96°^	79 ± 14#	7584

[a] The statistical significance for cell responsiveness (% responsive cells) was assessed using the χ^2 test: significantly different from Ca–CPPs (°, $p < 0.005$); from digested Ca–CPPs (^, $p < 0.005$). The variations in the average single-cell intracellular calcium concentration ($\Delta[Ca^{2+}]_i$) were analyzed by Student's *t*-test (*significantly different from Ca–CPPs, $p < 0.01$); from digested Ca–CPPs (#, $p < 0.01$). Each value represents the mean ± SD of 6–8 analogous experiments for at least 500 analyzed cells. Details of the calculations are reported in the Materials and methods section.

As far as the structure of (CPP + calcium) aggregates is concerned, two levels have been identified: a large-scale structure, some hundreds of nm in size (the peptide matrix), and a small substructure, more ramified, with fractal or entangled chain-like conformation typical of polycondensates. Although apparently similar, this internal structure is quite different from that found for whole-casein, the parent protein, that arranges as a network with reticulated amorphous calcium–phosphate nanoclusters,[42] modelled as oblate ellipsoids.[43] We underline that in the CPP solutions used here, the phosphate groups are

just those belonging to the phosphorylated serines of CPPs, thus in equimolar ratio with serine residues, see the Materials and methods section. No additional phosphate ions are present. Moreover, CPP chains are shorter than those of casein, and the fraction of serine residues in Ca–CPP is higher than that for casein (10.3% *vs.* 6.1% w/w).[24] Aggregation does not take place in the absence of Ca ions[9] and supramolecular organization of the CPP chains is promoted by divalent calcium ions, coordinating different phosphoserine residues belonging to the same or to different chains.

As expected, and as observed also in casein micelles at varying pH,[44] digestion modifies the CPP aggregates on both overall and local scales. On the large scale, CPP aggregates reduce in size upon digestion, but are still present. Peptides are fragments of casein, and their ability to form aggregates seems to be preserved, more than for casein. At pH 2, simulating the gastric step, the charges on the peptide chains, including those of the phosphoserine residues, are neutralized, as in casein. Charge interaction with calcium ions is lost. The size distribution of aggregates shifts towards small structures (a few tens of nm) that correspond to oligomers, possibly stabilized also by hydrophobic interactions. As the pH is raised, simulating the following intestinal step, large aggregates quickly reform, since the condensation nuclei are still present. In fact, on the local scale an entangled substructure is preserved throughout the process of digestion, as inferred from X-ray results (Fig. 3). The effect of acidification and enzyme action on this internal substructure of the aggregates shows up as a decrease in the radius of gyration of the subchains, connected to the characteristic distance between calcium complexation sites. Those findings indicate that complexation sites and the embedded calcium become more finely distributed in the peptide matrix. This fully agrees with the mass spectrometry result, revealing an increased fragmentation of CPPs upon *in vitro* digestion, moving the CPP distribution towards shorter peptides, mostly carrying one or more phosphoserines. Then, they preserve their ability to bind calcium in a mesh of smaller size.

From the structural point of view, then, digestion preserves the presence of supramolecular complexes, their size being still suitable to promote calcium internalization by intestinal cells. Moreover, digestion renders CPP aggregates more homogeneous-inside, dispersing condensation sites and disordering the network structure.

From the biological point of view we separately discussed results obtained using Ca–CPPs or Ca–dekCPPs in our cell intestinal human models.

Caco2 and HT-29 cells share the same origin from human colon adenocarcinoma, but, when differentiated, they acquire new features as described in detail,[45] such as the brush border associated hydrolases and structures which make them more similar to the cells of the small intestine. Nonetheless, some differences are still present. First of all, in strict connection to the tumoral origin of these cells, they display a high glucose consumption rate and glycogen accumulation. Second, the lack of lactase in HT-29 cells and of maltase-glucoamylase in both cell types make them different from the colon, where hydrolases are not present, but also from the small intestine. Still, due to the difficulties encountered in using *in vitro* primary cultures of bioptic intestinal fragments, HT-29 and Caco2 are considered suitable models and are the most used cell lines for studies of drug transport and/or cell toxicity. Known differences in the morphology and function of the two cell populations are present, depending on the cell culture and differentiation protocol, which permits to choose one cell line rather than the other, based on the research target.

In this regard, differentiated Caco2 cells, which constitute a monolayer of mainly absorptive epithelium, resemble the duodenum cells,[45] where the percentage of goblet cells reaches only 10%, as supported by a higher sucrase–isomaltase activity as compared to HT-29 cells.[9,31,46] Besides, they show that, by a higher presence of digestive enzymes[47] as it appears for the duodenum, the intestinal tract is more involved in the digestion of food. Even the presence of transporters like the TRPV6 channel,[12] indicative of the transcellular calcium absorption as the main pathway, as it was observed in duodenum,[48] together with the absence of L-type calcium channels, more typical of jejunum and ileum, where calcium is absorbed *via* a paracellular route, indicates that Caco2 cells are reasonable representatives of duodenum like cells.[48]

HT-29 cells, instead, present features of a more heterogeneous population with a minor proportion of the absorptive phenotype, together with a minor level of digestive enzymes.[47] These cells are characterized also by the presence of L-type calcium channels[11] and by a major permeability of their junctions, all signs of a higher level of absorption processes characteristic of the jejunum and ileum tracts.

Despite the limitations associated with the use of the described cell lines as a model of the human intestine, they have been preferred in place of other methods. In fact, a different possibility to study the CPP efficacy on calcium uptake by the intestine could be the Ussing Chamber, which is useful to monitor a passage of substance. In this sense, preliminary experiments have used the everted distal small intestine of rats demonstrating a positive effect exerted by CPPs in dependence of the CPP/calcium ratio.[49] The choice to use both cell lines lies in the possibility to distinguish between the two different principal mechanisms for calcium uptake activated by CPPs as demonstrated in previous studies.[11,12]

4.1. Ca–CPPs

The first important result is that digestion of Ca–CPP aggregates leads to an increased uptake of calcium ions in intestinal cells, both Caco2 and HT-29, with an impressive eight-fold improvement in Caco2 cells. Improved bioactivity may be due to the modulation of the interaction between Ca–CPP aggregates and the cell surface, for instance the type and duration of contact between aggregates and cells; besides, solubility may improve calcium availability. The increased bioavailability, after digestion, of the calcium associated with Ca–CPPs is evident, as both types of cells display an increase in calcium

uptake, a feature dependent both on the mechanism of interaction with cells and on the amount or the distribution of calcium within the complexes. Optimized dispersion of calcium within digested Ca–CPPs, as revealed by SAXS, can predispose for a higher solubility, and thus availability, of the mineral. Concerning the complicated interaction between the aggregates and the cell membrane, it may reasonably depend on the structural properties of the Ca–CPP complexes. Again, a plausible softening of digested Ca–CPP complexes, displaying a less rigid conformation with respect to the undigested ones, as revealed by SAXS, may promote better interaction with the cell membrane surface.

Comparison between the two cell lines, Caco2 and HT-29, can give some hint.

Both cell lines give a better response to digested Ca–CPPs with respect to the undigested complexes, but the huge enhancement (eight times more) induced in Caco2 cells, to be compared with the two-fold enhancement induced in HT-29 cells, is the most astonishing result. Let us then consider the two main mechanisms through which CPPs trigger the uptake of calcium: mainly *via* the TRPV6 channel, thus transcellular, regulated by vitamin D, in Caco 2 cells,[12] and *via* the depolarizing L-type calcium channels, thus paracellular, not vitamin D regulated, in HT-29 cells.[10] *In vivo*, transcellular calcium absorption takes place in the duodenum, according to a saturable kinetics, when the extracellular calcium concentration is low. Reversely, paracellular calcium absorption takes place in the distal jejunum and ileum when the extracellular calcium concentration is very high, for instance after a meal.[48]

In the case of Caco2 cells, morphologically and functionally very similar to the duodenum cells,[12] the huge enhancement in calcium uptake when treated with the digested Ca–CPP complexes as compared to the undigested homologues is mainly due to the ~5-fold increase in the fraction of responding cells, each one roughly doubling the amount of internalized calcium (see Table 2). It can be hypothesized that Ca–CPP rearrangement following digestion increases the amount of finely dispersed, slowly supplied, complexed calcium (thus improving the single-cell calcium uptake), meanwhile reducing the amount of free calcium responsible of the downregulation of TRPV6,[11] thus raising the number of responding cells.

In the case of HT-29 cells, very similar to the jejunum and ileum cells,[11] the percentage of responsive cells to Ca–CPPs is very high, already in the presence of the undigested form. This is expected for a mechanism devoted to massive calcium recovery, in abundance of calcium, both CPP-bound and free in solution. Digestion, reasonably, mainly affects the amount of calcium taken up by single cells, rather than the already huge number of responsive cells (see Table 3). Again, an increase in the fraction of complexed calcium (the most bioactive form) can be at the basis of the uptake efficiency improvement.

4.2. Ca–dekCPPs

Differently from Ca–CPPs, Ca–dekCPPs are very sensitive to the extracellular calcium concentrations, as they recruit all of the available calcium ions, while forming the bioactive aggregates.[24] As compared to Ca–CPPs, Ca–dekCPPs, with a less defined internal structure, display a higher capacity for promoting calcium uptake in both types of cells, in the undigested form. In Caco2 cells, this could be due to the effectiveness of dekCPPs in subtracting free calcium ions from the extracellular space, with a smaller downregulation of the TRPV6 channel. In HT-29 cells, more calcium bound to bioactive dekCPP aggregates, as compared to the Ca–CPPs, is reflected in higher calcium uptake. Interestingly, and opposite to Ca–CPPs, digestion reduces this ability. The instability of the Ca–dekCPP complexes is likely to be at the basis of their reduced performance. In Caco2 cells the responsiveness decreases to a value similar to that observed when undigested Ca–CPPs are administered, probably for an increased downregulation of the TRPV6 channel due to a higher amount of calcium ions freed from a labile Ca–dekCPP matrix. Accordingly, in HT-29 cells, the reduction in calcium uptake indicates a lowering in the calcium content of the most bioactive CPP complexes. The modification of the CPP complexes operated by digestion and its effect on the interaction with the cell membranes are also evident from the enhanced heterogeneity in the time course profiles of the intracellular calcium concentration in digested dekCPPs.

The CPP mixture we addressed in the present and previous studies is a preparation purified from bovine casein.

The formation of CPPs from casein digestion is an issue much addressed in many studies. It has been shown to occur *in vitro*, from the digestion of skim milk[16] and/or from milk based infant formula digestion[4] or from milk fruit beverages,[50] and also, most importantly, *in vivo* with the detection of CPPs in human plasma following digestion of milk and yogurt[6] as well as in the distal ileostomy fluid.[51] Nonetheless, the possibility that, after a dairy meal, aggregates of CPPs and calcium can be formed at the optimal conformation and molar ratio, such as the ones described above, and therefore bioactive after the modification induced by the digestion, and high-performing, is a desirable issue, but unfortunately unrealistic. In fact, two main aspects have to be considered: (a) the probability that biologically active casein phosphopeptides do originate and in appreciable amounts after digestion, (b) different food matrix and physiological conditions, such as digestion efficiency, can produce every time different types of peptides. In addition, *in vitro* digestion does not result in the same exact peptides as *in vivo* digestion, since factors like food matrix, environmental conditions, and physiological alteration, can modulate the efficiency and thus the product of digestion. Besides, the digestion of dairy products by infants, due to the incomplete pool of proteases of their immature gastrointestinal apparatus,[52] can originate peptides with different structures and bioactivity as compared to adults.

An optimized formulation for extra calcium supply with easy delivery could then be employed for those segments of population, as children or seniors, with a higher demand for the mineral, or in the presence of pathological conditions such as osteoporosis.

5. Conclusion

Data presented here demonstrate for the first time that after digestion pre-formed (CPP + Ca) aggregates still maintain their conformation and retain their bioactivity as promoters of calcium uptake in intestinal cells. The employment of purified CPPs pre-complexed with calcium ions proved to be fundamental, as it prevents problems occurring when casein hydrolysis results in uncontrolled mixtures of CPPs. Besides, this choice is instrumental to bioactivity, due to the bioavailability of the mineral and the stability of aggregates. Apart from numerical values, always digestion of complexes has proved to enhance calcium uptake, whatever their mechanism of interaction with plasma membranes, TRPV6 in Caco2 cells and depolarizing L-type calcium channels in HT-29 cells. Thus, a CPP formulation with the features described here, administered as dietary supplements, stands as a promising tool for calcium delivery. Its efficiency is likely to be higher than when incorporated in the form of ingredients into traditional and/or novel foods, the release from food matrix and the digestion survival being possible limiting factors. Meanwhile the ease of administration is kept. In conclusion, results presented here strengthen the possibility of considering CPP-based calcium vectors as nutraceuticals or supplements to be employed in every situation requiring high calcium absorption.

Acknowledgements

We thank T. Narayanan for his precious support at the ESRF ID02 beamline and for useful discussions.

References

1 R. Nagpal, P. Behare, R. Rana, A. Kumar, M. Kumar, S. Arora, F. Morotta, S. Jain and H. Yadav, *Food Funct.*, 2011, **2**, 18–27.
2 H. Korhonen, *J. Funct. Foods*, 2009, **1**, 177–187.
3 M. J. Garcia-Nebot, A. Alegria, R. Barbera, M. Del Mar Contreras and I. Recio, *Peptides*, 2010, **31**, 555–561.
4 E. Miquel, J. A. Gomez, A. Alegria, R. Barbera, R. Farré and I. Recio, *J. Agric. Food Chem.*, 2005, **53**, 3426–3433.
5 G. Picariello, P. Ferranti, O. Fierro, G. Mamone, S. Caira, A. Di Luccia, S. Monica and F. Addeo, *J. Chromatogr., B: Biomed. Appl.*, 2010, **878**, 2956–2308.
6 B. Chabance, P. Marteau, J. C. Rambaud, D. Migliore-Samour, M. Boynard, P. Perrotin, R. Guillet, P. Jollès and A. M. Fiat, *Biochimie*, 1998, **80**, 155–165.
7 R. Boutrou, C. Gaudichon, D. Dupont, J. Jardin, G. Airinei, A. Marsset-Baglieri, R. Benamouzig, D. Tomé and J. Leonil, *Am. J. Clin. Nutr.*, 2013, **97**, 1314–1323.
8 R. Berrocal, S. Chanton, M. A. Juillerat, B. Pavillard, J. C. Scherz and R. Jost, *J. Dairy Res.*, 1989, **56**, 335–341.
9 C. Gravaghi, E. Del Favero, L. Cantu, E. Donetti, M. Bedoni, A. Fiorilli, G. Tettamanti and A. Ferraretto, *FEBS J.*, 2007, **274**, 4999–5011.
10 S. Cosentino, C. Gravaghi, E. Donetti, B. M. Donida, G. Lombardi, M. Bedoni, A. Fiorilli, G. Tettamanti and A. Ferraretto, *J. Nutr. Biochem.*, 2010, **21**, 247–254.
11 S. Perego, S. Cosentino, A. Fiorilli, G. Tettamanti and A. Ferraretto, *J. Nutr. Biochem.*, 2012, **23**, 808–816.
12 S. Perego, A. Zabeo, E. Marasco, P. Giussani, A. Fiorilli, G. Tettamanti and A. Ferraretto, *J. Funct. Foods*, 2013, **5**, 847–857.
13 L. Munaron, S. Antoniotti, A. Fiorio Pla and D. Lovisolo, *Curr. Med. Chem.*, 2004, **11**, 1533–1543.
14 S. C. Wright, J. Zhong and J. W. Larrick, *FASEB J.*, 1994, **8**, 654–660.
15 J. M. Brown and L. D. Attardi, *Nat. Rev. Cancer*, 2005, **5**, 231–237.
16 T. Ono, Y. Takagi and I. Kunishi, *Biosci., Biotechnol., Biochem.*, 1998, **62**, 16–21.
17 M. Hansen, B. Sandstörm, M. Jensen and S. S. Sørensen, *J. Pediatr. Gastroenterol. Nutr.*, 1997, **24**, 56–62.
18 M. Hansen, B. Sandstørm, M. Jensen and S. S. Sørensen, *J. Trace Elem. Med. Biol.*, 1997, **11**, 143–149.
19 M. Hansen, B. Sandström and B. Lönnerdal, *Pediatr. Res.*, 1996, **40**, 547–552.
20 H. Tsuchita, T. Goto, T. Shimizu, Y. Yonehara and T. Kuwata, *J. Nutr.*, 1996, **126**, 86–93.
21 H. W. Jerber and R. Jost, *Calcif. Tissue Int.*, 1986, **38**, 350–357.
22 E. C. Reynolds, *USA Patent*, 5, 015, 628, 1991.
23 E. C. Reynolds, C. J. Cain, L. F. Webber, C. L. Black, P. F. Riley, I. H. Johnson and J. W. Perich, *J. Dent. Res.*, 1995, **74**, 1272–1279.
24 S. Cosentino, B. M. Donida, E. Marasco, E. Del Favero, L. Cantù, G. Lombardi, A. Colombini, S. Iametti, S. Valaperta, A. Fiorilli, G. Tettamanti and A. Ferraretto, *Int. Dairy J.*, 2010, **20**, 770–776.
25 F. Bronner, D. Pansu and W. D. Stein, *Am. J. Physiol.*, 1986, **250**, G561–G569.
26 K. H. Ellegard, C. Gammelgard-Larsen, E. S. Sorensen and S. Fedosov, *Int. Dairy J.*, 1999, **9**, 639–652.
27 M. Jovaní, R. Barberá, R. Farré and E. Martin de Aquilera, *J. Agric. Food Chem.*, 2001, **49**, 3480–3485.
28 N. Ortega, J. Reguant, M. P. Romero, A. Macià and M. J. Motilva, *J. Agric. Food Chem.*, 2009, **57**, 5743–5749.
29 O. H. Lowry, N. J. Rosebrough, A. L. Farr and R. J. Randall, *J. Biol. Chem.*, 1951, **193**, 265–275.
30 J. S. Pedersen, in *Neutrons, X-Ray and Light*, ed. P. Lindner and T. Zemb, North-Holland Elsevier, Amsterdam, 2002, pp. 391–420.
31 A. Bouchoux, G. Gésan-Guiziou, J. Pérez and B. Cabane, *Biophys. J.*, 2010, **99**, 3754–3762.
32 A. Ferraretto, C. Gravaghi, E. Donetti, S. Cosentino, B. M. Donida, M. Bedoni, G. Lombardi, A. Fiorilli and G. Tettamanti, *Anticancer Res.*, 2007, **27**, 3919–3925.

33 M. Hekmati, S. Polak-Charcon and Y. Ben-Shaul, *Cell Differ. Dev.*, 1990, **31**, 207–218.
34 A. Ferraretto, A. Signorile, C. Gravaghi, A. Fiorilli and G. Tettamanti, *J. Nutr.*, 2001, **131**, 1655–1661.
35 G. Grynkiewicz, M. Poenie and R. Y. Tsien, *J. Biol. Chem.*, 1985, **260**, 3440–3450.
36 C. G. De Kruif, T. Huppertz, V. S. Urban and A. V. Petukhov, *Adv. Colloid Interface Sci.*, 2012, **171–172**, 36–52.
37 D. G. Dalgleish, *Soft Matter*, 2011, **7**, 2265–2272.
38 D. J. McMahon and B. S. Oommen, *J. Dairy Sci.*, 2008, **91**, 1709–1721.
39 F. Pignon, G. Belina, T. Narayanan, X. Paubel, A. Magnin and G. Gésan-Guiziou, *J. Chem. Phys.*, 2004, **121**, 8138–8146.
40 C. Holt, C. G. De Kruif, R. Tuinier and P. A. Timmins, *Colloids Surf., A*, 2003, **213**, 275–284.
41 C. Ekmekcioglu, *Food Chem.*, 2002, **76**, 225–230.
42 C. Holt, *Curr. Opin. Struct. Biol.*, 2013, **23**, 420–425.
43 A. Shukla, T. Narayanan and D. Zanchi, *Soft Matter*, 2009, **5**, 2884–2888.
44 C. Moitzi, A. Menzel, P. Schurtenberger and A. Stradner, *Langmuir*, 2011, **27**, 2195–2203.
45 A. Zweibaum, M. Laburthe, E. Grasset and D. Louvard, in *Handbook of physiology*, Am. Phys. Soc., Bethesda, MD, 4th edn, 1991, vol. 7, pp. 223–255.
46 J. L. Madara, J. S. Trier and R. Johnson, in *Physiology of the Gastrointestinal Tract*, Raven Press, New York, 2nd edn, 1987, 1209–1249.
47 A. Quaroni and J. Hochman, *Adv. Drug Delivery Rev.*, 1996, **22**, 3–52.
48 G. L. Kellett, *Nutr. Rev.*, 2011, **69**, 347–370.
49 D. Erba, S. Ciappellano and G. Testolin, *Nutrition*, 2002, **18**(9), 743–746.
50 M. J. García-Nebot, A. Alegría, R. Barberá, M. del Mar Contreras and I. Recio, *Peptides*, 2010, **31**, 555–561.
51 H. Meisel, H. Bernard, S. Fairweather-Tait, R. J. FitzGerald, R. Hartmann, C. N. Lane, D. McDonagh, B. Teucher and J. M. Wal, *Br. J. Nutr.*, 2003, **89**, 351–358.
52 M. J. Henschel, M. J. Newport and V. Parmar, *Biol. Neonate*, 1987, **52**, 268–272.